

Online Supplementary Material

Appendices to *Looking for compensation at multiple scales in a wetland bird community*. Barraquand F., Picoche C., Aluome C., Carassou L., and Feigné C.

Appendix S1 - List of species

Among the 279 bird species which were observed throughout the monitoring, we focused on 2 functional groups (ducks and waders) and 2 groups of phylogenetically close species (Anatini, Calidris) described in Table 1. In Table 2, we also present the most frequent birds present with the species we consider. The rest of the community (not detailed here) amount to 1% of the total number of observed birds.

Functional group	Species	Name	% occurrence	% abundance
Ducks	<i>Anas acuta</i>	Northern pintail	59.9	1.708
	<i>AnasSpatula clypeata</i>	Northern shoveler	63.5	1.580
	<i>Anas crecca</i>	Eurasian teal	64.2	6.614
	<i>AnasMareca penelope</i>	Eurasian wigeon	36.5	0.055
	<i>Anas platyrhynchos</i>	Mallard	63.8	3.388
	<i>AnasSpatula querquedula</i>	Garganey	26.0	0.032
	<i>AnasMareca strepera</i>	Gadwall	48.7	0.308
	<i>Anser anser</i>	Greylag goose	47.3	1.135
	<i>Aythya ferina</i>	Common pochard	57.1	1.053
	<i>Aythya fuligula</i>	Tufted duck	45.8	0.467
	<i>Aythya marila</i>	Greater scaup	6.5	0.005
	<i>Branta bernicla</i>	Brant	2.3	0.001
	<i>Branta canadensis</i>	Canada goose	5.1	0.002
	<i>Cygnus olor</i>	Mute swan	50.0	0.618
	<i>Fulica atra</i>	Eurasian coot	64.3	16.007
	<i>Netta rufina</i>	Red-crested pochard	27.0	0.030
	<i>Tadorna tadorna</i>	Common shelduck	53.1	0.870
Waders	<i>Actitis hypoleucos</i>	Common sandpiper	25.3	0.054
	<i>Arenaria interpres</i>	Ruddy turnstone	14.7	0.020
	<i>Calidris alba</i>	Sanderling	4.1	0.004
	<i>Calidris alpina</i>	Dunlin	37.2	26.394
	<i>Calidris canutus</i>	Red knot	22.6	0.406
	<i>Calidris ferruginea</i>	Curlew sandpiper	14.8	0.067
	<i>Calidris minuta</i>	Little stint	25.1	0.129
	<i>Calidris temminckii</i>	Temminck's stint	4.6	0.001
	<i>Charadrius dubius</i>	Little ringed plover	18.2	0.040
	<i>Charadrius hiaticula</i>	Common ringed plover	34.2	0.921
	<i>Gallinago gallinago</i>	Common snipe	23.1	0.184
	<i>Himantopus himantopus</i>	Black-winged stilt	12.1	0.079
	<i>Limosa lapponica</i>	Bar-tailed godwit	18.4	0.327
	<i>Limosa limosa</i>	Black-tailed godwit	29.7	1.802
	<i>Numenius arquata</i>	Eurasian curlew	17.0	1.167
	<i>Numenius phaeopus</i>	Whimbrel	11.1	0.102
	<i>PhilomachusCalidris pugnax</i>	Ruff	11.4	0.010
	<i>Pluvialis apricaria</i>	European golden plover	5.0	0.002
	<i>Pluvialis squatarola</i>	Grey plover	32.9	0.669
	<i>Recurvirostra avosetta</i>	Pied avocet	25.0	0.775
	<i>Tringa erythropus</i>	Spotted redshank	23.9	0.133
	<i>Tringa glareola</i>	Wood sandpiper	9.6	0.008
	<i>Tringa nebularia</i>	Common greenshank	25.0	0.173
	<i>Tringa ochropus</i>	Green sandpiper	15.4	0.014
	<i>Tringa totanus</i>	Common redshank	32.4	0.670
	<i>Vanellus vanellus</i>	Northern lapwing	22.8	0.265

Table 1: Composition of the two functional groups considered in the manuscript. The genera on which we focused inside these functional groups are coloured in the table. The percentage of occurrences correspond to the number of dates when a species was observed, compared to the total number of observation dates. The percentage of abundances correspond to the ratio of the abundance of a given species on the total abundance of all birds observed during the monitoring.

Functional group	Species	Name	% occurrence	% abundance
Other	Accipiter nisus	Eurasian sparrowhawk	12.8	0.003
	Alcedo atthis	Common kingfisher	12.1	0.017
	Ardea cinerea	Grey heron	63.1	2.480
	Bubulcus ibis	Western cattle egret	37.9	0.381
	Casmerodius albus Ardea alba	Great egret	30.0	0.150
	Chroicocephalus ridibundus	Black-headed gull	51.3	9.645
	Ciconia ciconia	White stork	51.3	0.905
	Circus aeruginosus	Western marsh harrier	23.3	0.017
	Egretta garzetta	Little egret	55.1	6.511
	Falco peregrinus	Peregrine falcon	13.8	0.003
	Gallinula chloropus	Common moorhen	42.2	1.106
	Larus argentatus	European herring gull	36.4	3.414
	Larus fuscus	Lesser black-backed gull	32.1	0.088
	Larus marinus	Great black-backed gull	38.9	0.039
	Larus michahellis	Yellow-legged gull	17.5	0.210
	Milvus migrans	Black kite	12.8	0.106
	Nycticorax nycticorax	Black-crowned night heron	58.4	0.160
	Phalacrocorax carbo	Great cormorant	57.7	3.616
	Platalea leucorodia	Eurasian spoonbill	48.2	0.720
	Podiceps cristatus	Great crested grebe	28.6	0.033
	Podiceps nigricollis	Black-necked grebe	12.0	0.008
	Rallus aquaticus	Water rail	40.4	0.594
	Tachybaptus ruficollis	Little grebe	44.8	0.403
	Threskiornis aethiopicus	African sacred ibis	12.5	0.019

Table 2: Most frequent birds (observed more than 75 times during the monitoring) which are not described in the previous functional groups (see previous legend for more details on the column signification).

Appendix S12 - Temporal patterns of in the Teich bird community

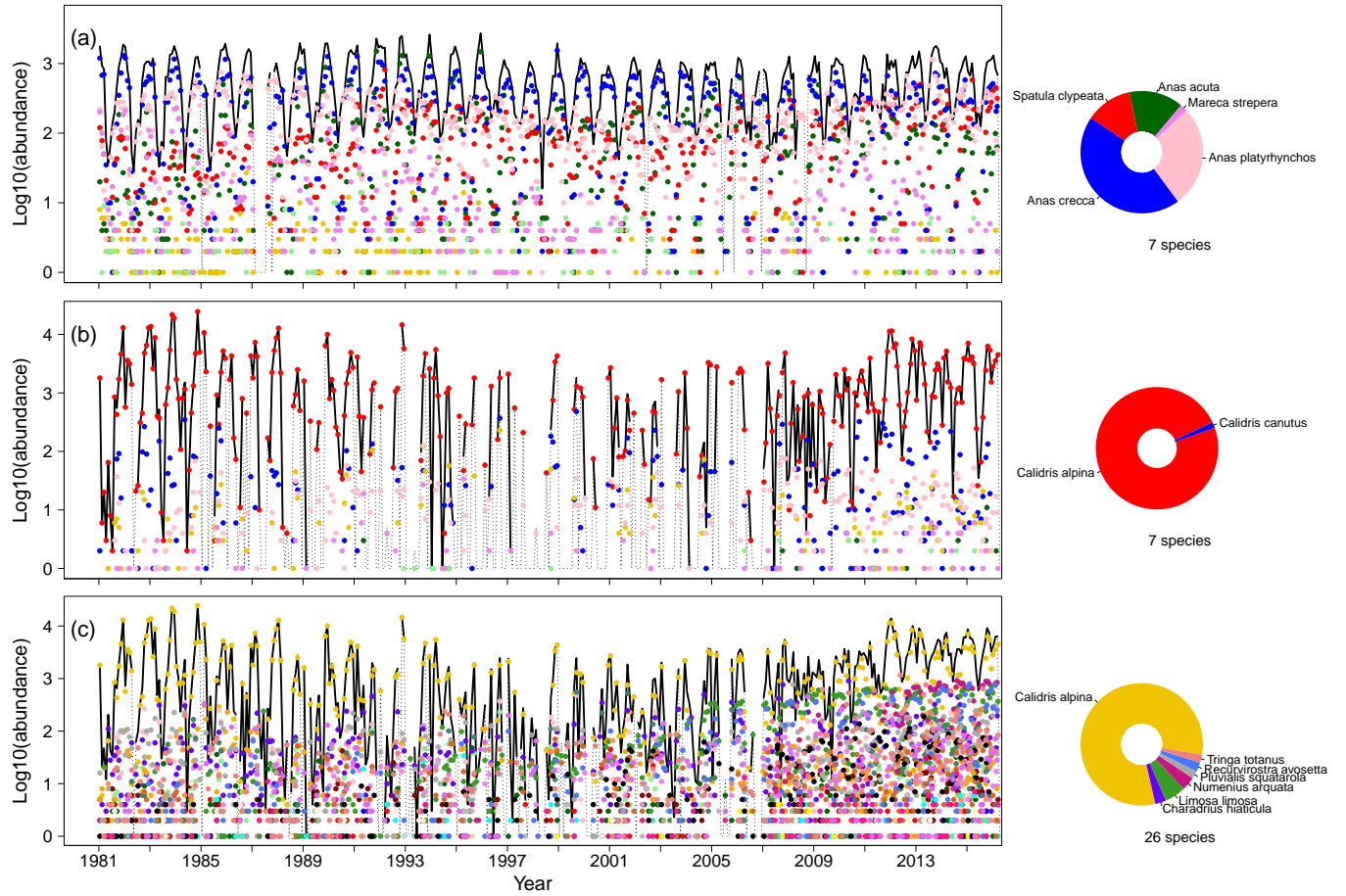


Figure S1: Time series of counts for ducks of the **genus tribe *Anas-tini*** (a), calidrids (b, *Calidris* genus), and all waders (c, including calidrids). The solid black lines represent trends in summed abundances for each guild when abundances are strictly positive, thin dotted lines connect positive to zero abundances. The coloured symbols below the curves represent each species abundances, with species composition on the right side on the donut plots for the most abundant species (over 1% of relative abundance in the group considered), **and total number of species taken into account in the group**.

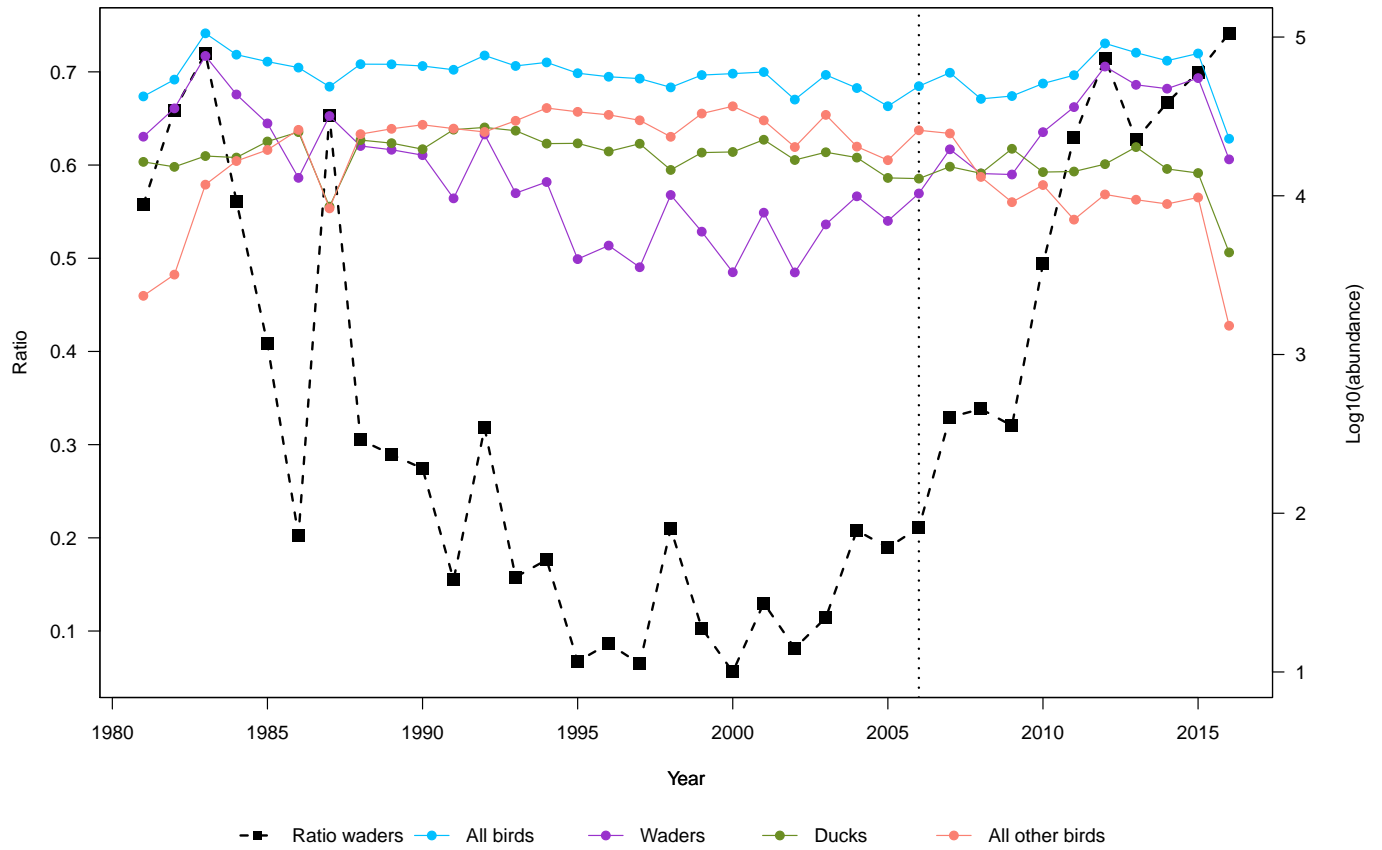


Figure S2: Temporal trends in the abundance of all birds and the main functional groups (waders and ducks), with one point per year. The duck category actually includes all species functionally similar to ducks (i.e., anatids and the common coot). The dashed line presents the ratio of wader individuals in the whole community, which changes over time.

Appendix S23 - Gross synchrony index at the whole community level

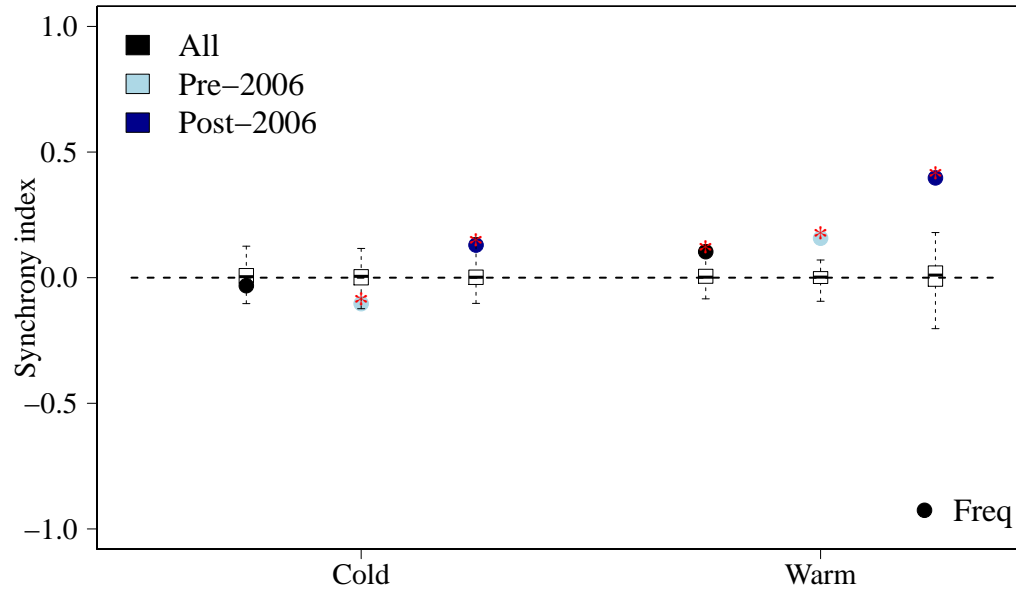


Figure S3: Gross' synchrony index as a function of the season (cold and warm seasons), calculated among the 60 most frequent species in the Teich reserve. The index was computed in each panel on the whole dataset (black) or using two periods: before and after 2006 (light and dark blue), the year of the change in water level management. Red stars correspond to synchrony values significantly different from the null model (independent species), at the Bonferroni-corrected 10% threshold.

Appendix S34 - Correlation in log-scale between cormorant and heron+egret

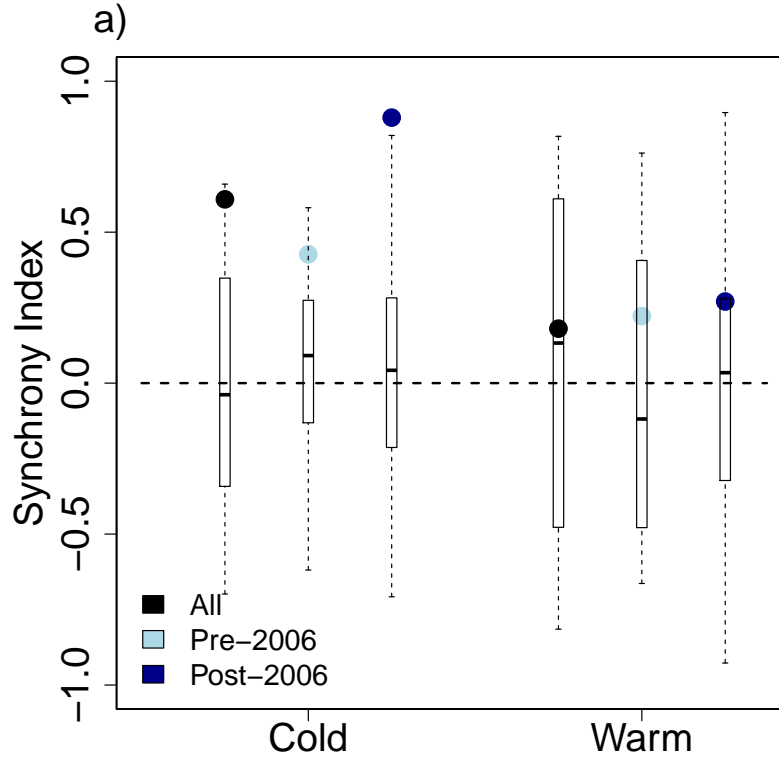


Figure S4: Gross' synchrony index as a function of the season (cold and warm seasons), calculated on log-transformed abundance data for the two groups formed by cormorant and heron+egret. The index was computed in each panel on the whole dataset (black) or using two periods: before and after 2006 (light and dark blue), the year of the change in water level management.

We noted on Fig. 4 in the main text that cormorants, herons and egrets seemed to compensate each other, at least for the first period of the time series. This compensation was seen on a log scale, and seemed conspicuous on that scale. We thus wondered if log-transforming the abundance would affect the values of the synchrony index observed for this group, and make compensation more likely. It appears to be the reverse: synchrony values are higher with log-transformed abundances.

Appendix S5 - Synchrony indices using biomasses

We used the mean mass of each species to compute the variation of observed biomasses and the corresponding synchrony indices. This did not change our conclusions.

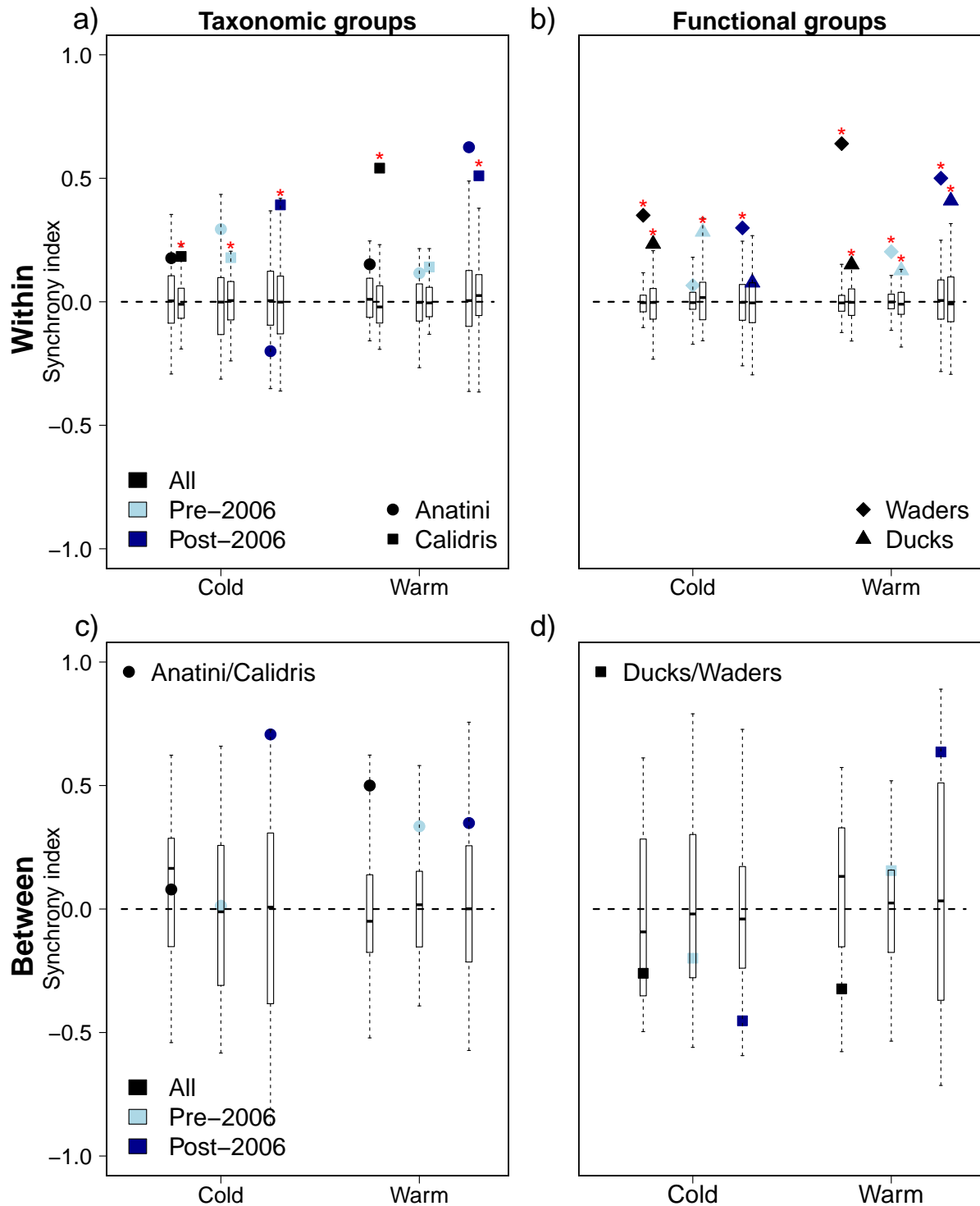


Figure S5: Gross' synchrony index (η) as a function of the season (cold and warm seasons), calculated within (top, a-b) and between (bottom, c-d) groups, using biomasses instead of abundances. The groups considered were different functional groups (ducks vs waders, right b-d) or taxonomic groups (*Anas* genus, *Calidris* genus, left a-b) groups. The index was computed in each panel on the whole dataset (black) or using two periods: before and after 2006 (light and dark blue), the year of the change in water level management. Boxplots indicate the distribution of η under the null hypothesis (independent species) and filled symbols correspond to the observed values. Red stars correspond to synchrony values significantly different from the null model, at the 10% threshold with a Benjamini-Hochberg correction

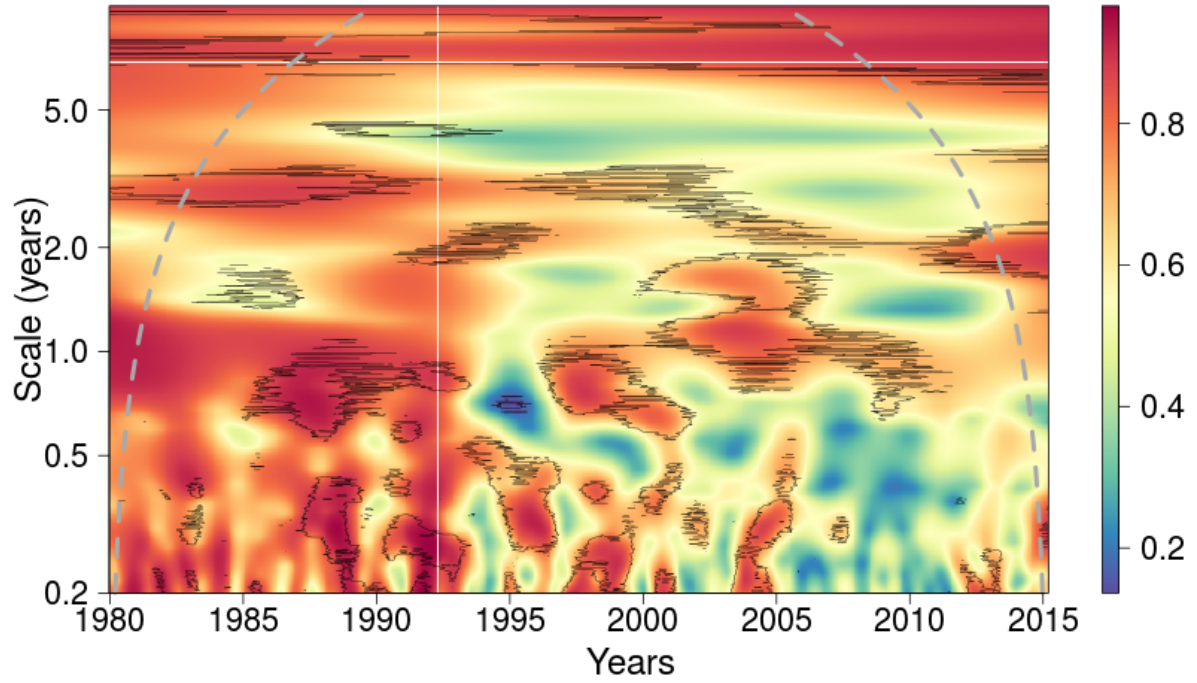


Figure S6: Wavelet modulus ratio for the wader community, scaling from 0 (compensation, blue color) to 1 (synchrony, red color), using the masses instead of the abundances of each species. Dashed black lines delineate regions significantly different from the null model (independently fluctuating species) with a false discovery rate controlled at the 10% threshold.

Appendix S64 - Properties of the Gross whole community synchrony index η when two groups react in opposite ways

Here, we make η vary with the number of species, richness of the community, and the strength of the effect of the environment. Starting from the model developed by Gross et al. [1] (developed in their Appendix D), we explored the effect of a shared environmental driver on a community formed by two groups reacting oppositely to this driver.

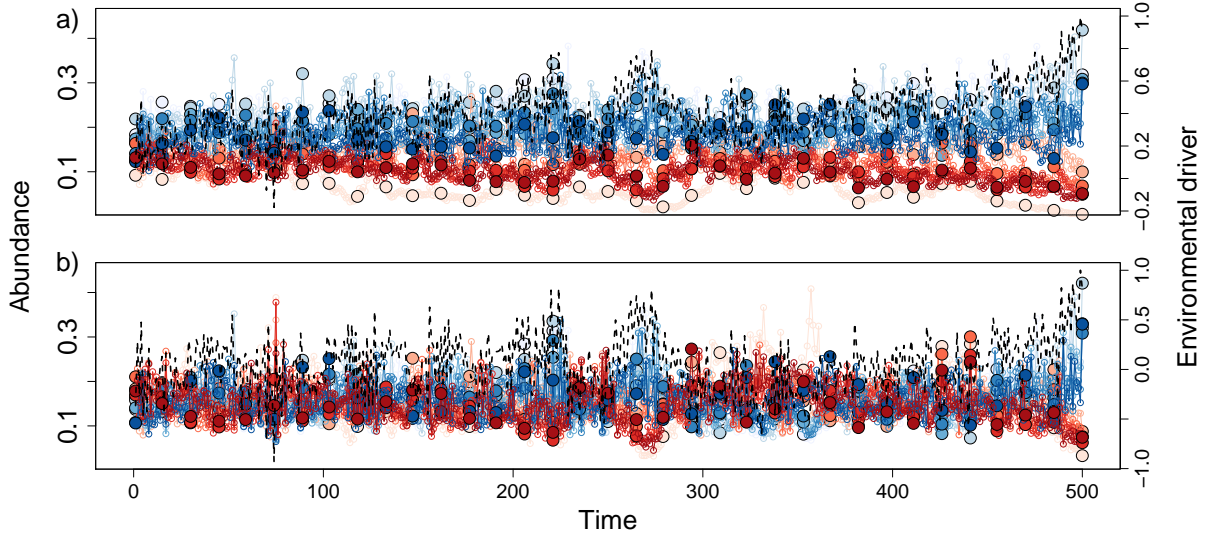


Figure S7: Time series for a community of 10 species, with a strong effect of the environment ($b=0.75$, see eq. 1) and a time series of 500 time steps. Open circles represent all points of the time series while large filled circles correspond to the sub-sampling of the time series (keeping only 35 points). Cold colors indicate species which react positively to the environmental signal and warm colors indicate species which have a negative reaction to the same signal. The environmental signal is shown in black, dashed lines, and indexed on the right axis. This signal either follows an increasing trend (a), or just an autocorrelated signal (b).

We assume that the environmental driver $U(t)$ is an autocorrelated signal (see below for details).

The dynamics of species i then follows the equation 1:

$$x_i(t+1) = x_i(t) \exp \left(r_i \left(1 - \frac{x_i(t) + \sum_{j \neq i}^n \alpha x_j(t)}{K} \right) + b_i U(t) + \epsilon_i(t) \right) \quad (1)$$

where the whole community is formed by $N = 2n$ species, with 2 groups of n species who have exactly opposite reaction to the environmental driver, that is $\forall i \in [1, n], \exists j \in [1, n], b_j = -b_i = b$. The growth rate r_i follows a normal distribution with mean 1 and standard deviation 0.25. All interaction coefficients α are set to 0.5 and $K = \frac{1+\alpha(N-1)}{N}$, to keep the model in other ways exactly similar to Gross et al. [1]. The noise $\epsilon_i(t)$ is normally distributed, centered on 0 with a standard deviation of 0.1.

We compared results for time series of length 35 (the length of our data set when computing η), 100 and 500. For all simulation experiments, the dynamics are first run for 500 time steps as a burn-in. To take into account different observational designs, we either take the first 35 or 100 time steps of the following 500-time steps series, or subsample the time series in order to get 35 or 100 time points (which removes some autocorrelation in the dynamics). We also considered several community richness (10, 30, 60 and 100 species), and several strengths of the response to the environmental signal ($b = [0.1, 0.5, 0.75]$). For each combination of parameters, we computed 10 repetitions (i.e., replicates).

We considered different types of environmental driver (simply autocorrelated or with a linear trend), crossed with subsampling / no subsampling as described above. We considered in total three scenarios, and present below how an increasing strength of response to the environment changes expectations for all three:

- Scenario 1: $U_t = u_t$ where u_t is an autocorrelated signal (standardized); no subsampling of the data

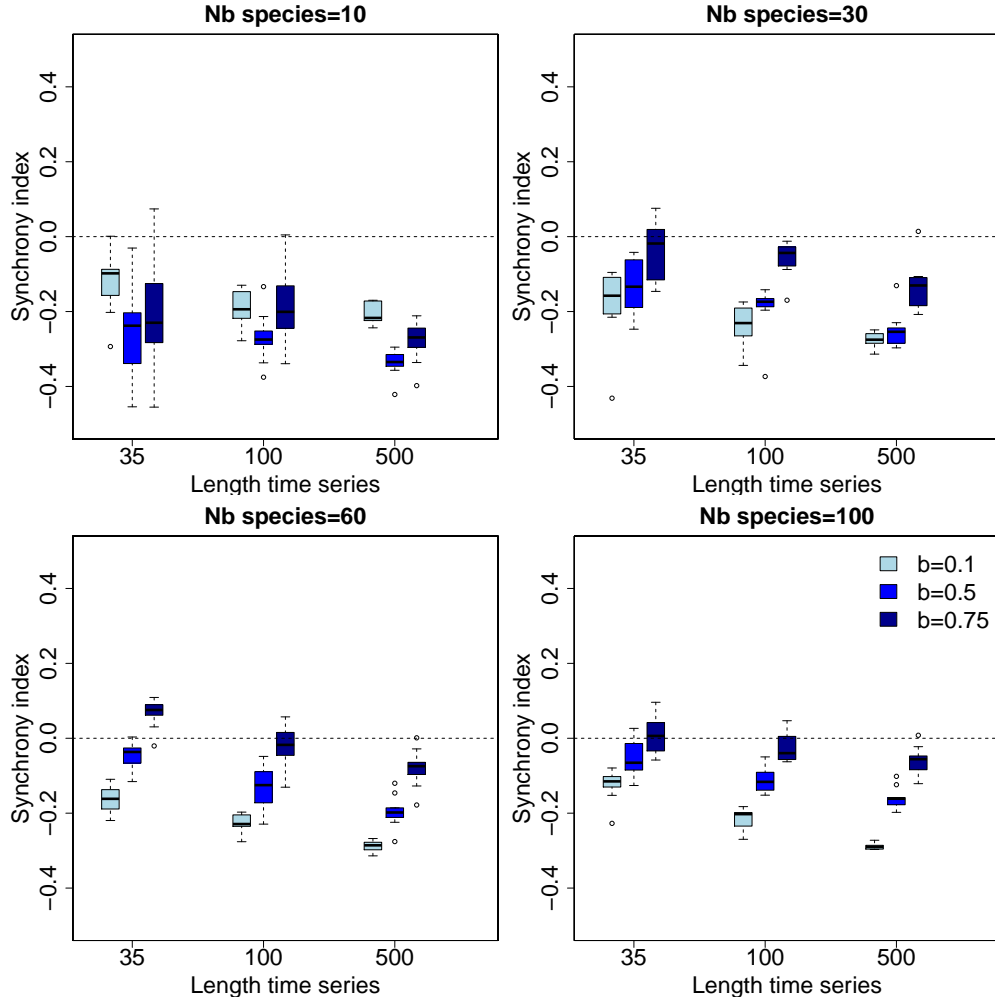


Figure S8: Evolution of Gross' synchrony index for different time series length and number of species in the community, in simulations where there is no trend in the environmental signal and the data is not subsampled, keeping the autocorrelation of the environment. The parameter b is the effect strength of the environmental variable.

- Scenario 2: $U_t = u_t$; data subsampling

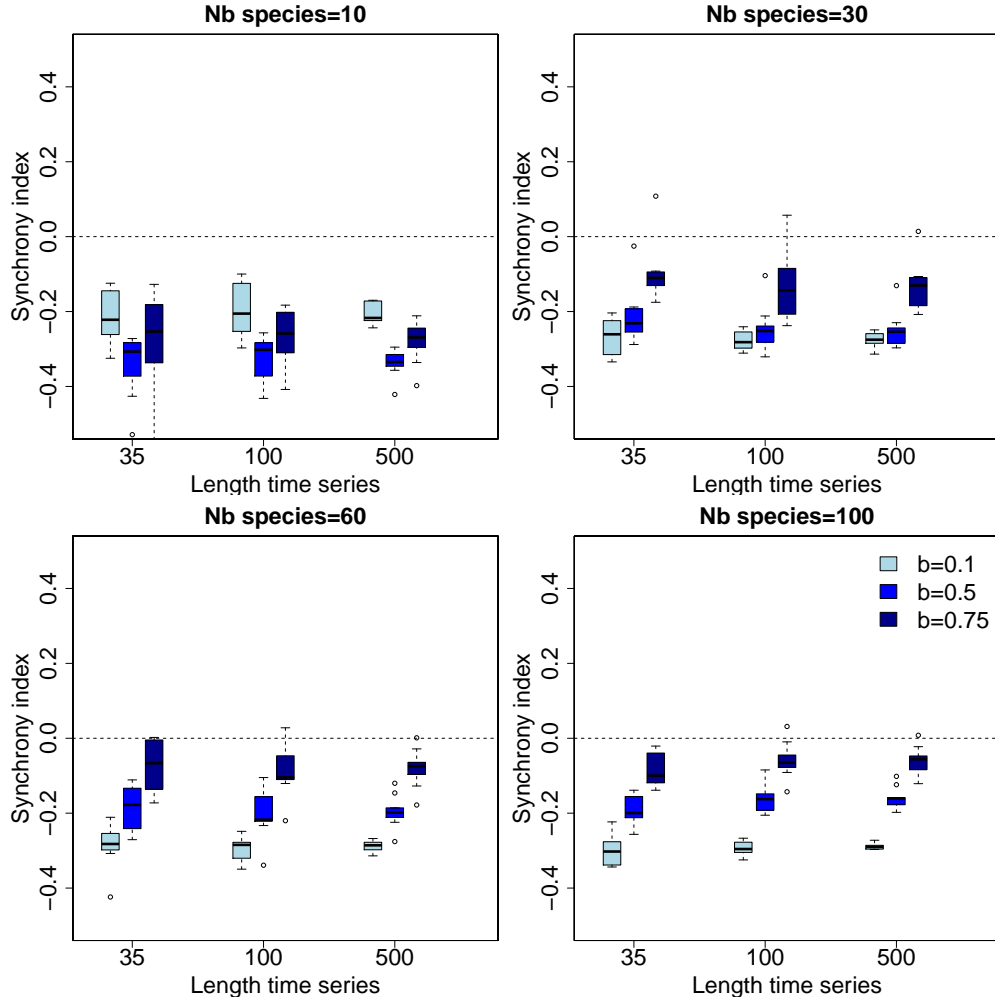


Figure S9: Gross' synchrony index for different time series length and number of species in the community, in simulations where there is no trend in the environmental signal and the data is subsampled (keeping 35 or 100 time steps), removing in effect the autocorrelation of the environment. **The parameter b is the effect strength of the environmental variable.**

- Scenario 3: $U_t = U_{\min} + (U_{\max} - U_{\min})(u_t + x_t)/2$ where $x_t \in [0, 1]$ follows an increasing trend; data subsampling

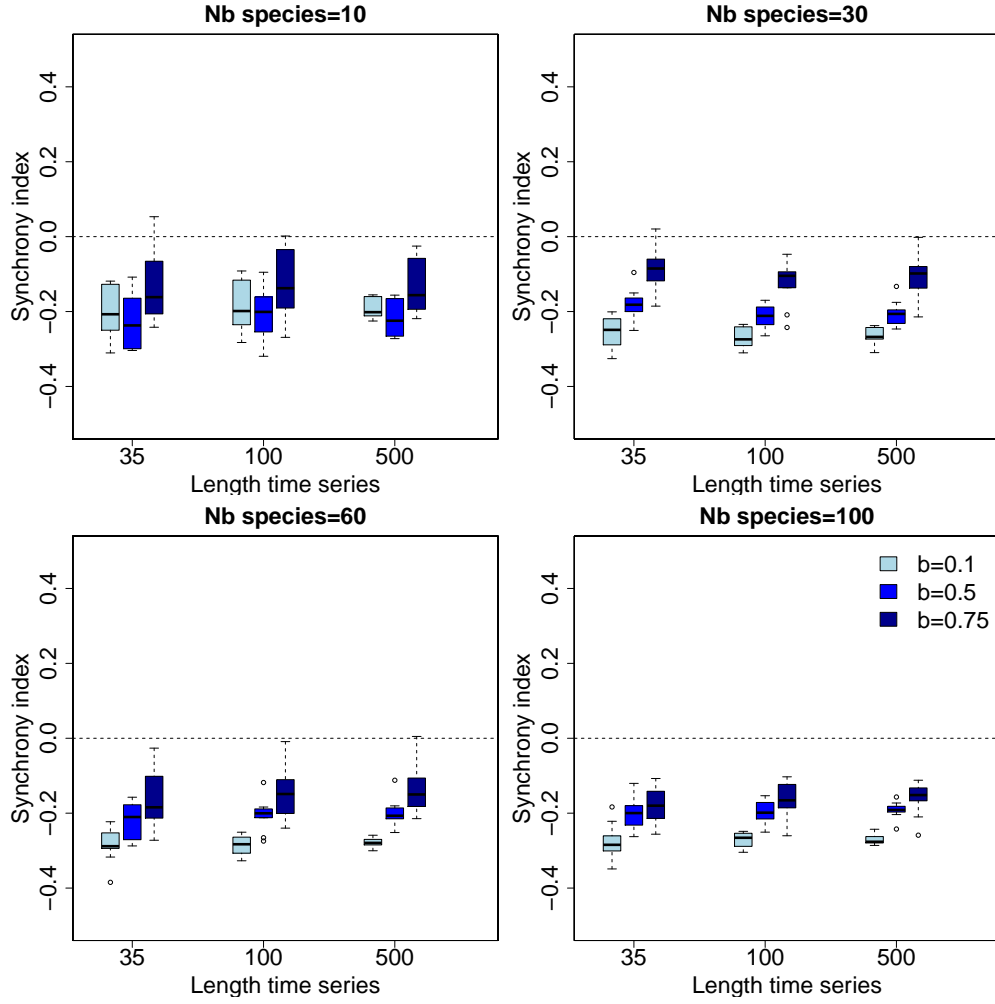


Figure S10: Gross' synchrony index for different time series length and number of species in the community, in simulations where there is an increasing trend in the environmental signal and the data is subsampled (for 35 or 100 time steps), removing part of the autocorrelation of the environment in the dynamics of the species. The parameter b is the effect strength of the environmental variable.

We first confirm that unless there is a very high temporal autocorrelation in the driver (as in Fig. S8), if we consider two groups which have opposite reactions to the same driver, the Gross index is not sensitive to the length of the time series or to the number of species in the community, in the sense that it will not indicate falsely synchrony. The main finding of these analyses, aside from the robustness of the η index, is that for large communities (over 10 species), synchrony is always higher when the response to the driver is stronger. Coming back to the interpretation of our results in the Teich reserve case, this means that the more bird population growth rates respond to changes in the water levels, the less we can expect compensation at the whole community level, even though compensation may be manifest at the functional group level (here,

the group of species responding similarly to the environmental variable).

Appendix S57 - Effect of “missing” values on wavelet analyses

We investigate here if exactly-zero abundances can distort the compensation patterns evidenced by the wavelet coherence. We chose a “worst case” simulation with 10% missing values for all species, and few species below that 10% level. The results show that while the statistical significance of the values can change (i.e., the data is more compatible with the null hypothesis of time series uncorrelated between species, assuming the null is true), the occurrence of compensation (blue values in Fig.S11) does not. The wavelet coherence index is therefore robust to the presence of zeroes in the time series.

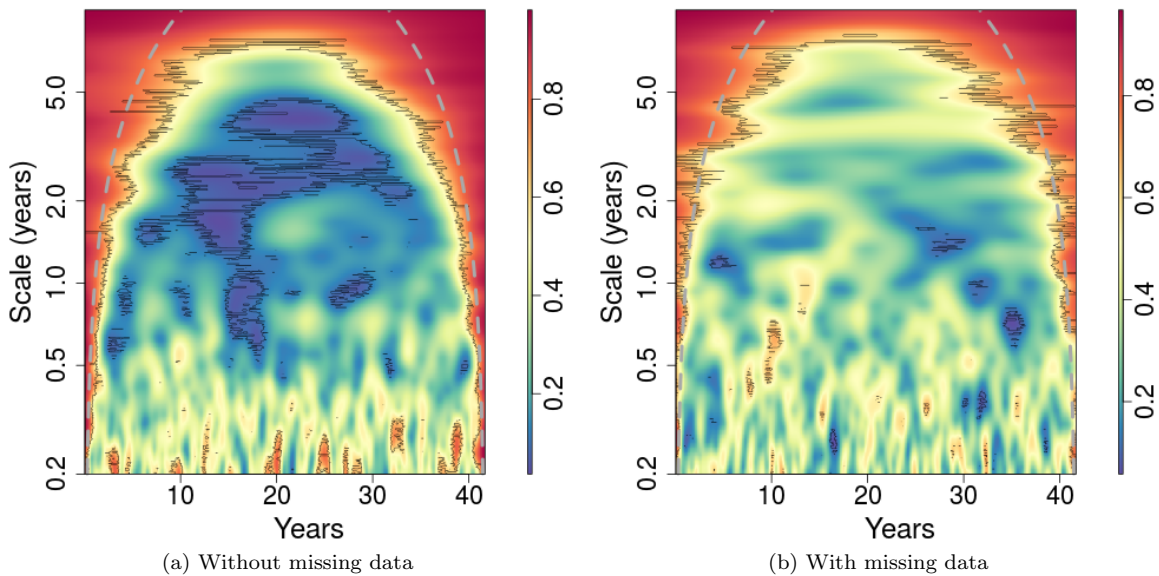


Figure S11: Wavelet coherence for a community with compensatory dynamics, without (a) and with (b) missing data

References

- [1] Gross, K., Cardinale, B. J., Fox, J. W., Gonzalez, A., Loreau, M., Wayne Polley, H., Reich, P. B. & van Ruijven, J., 2013 Species richness and the temporal stability of biomass production: a new analysis of recent biodiversity experiments. *The American Naturalist* **183**, 1–12.